Available online at www.sciencedirect.com

SciVerse ScienceDirect

www.elsevier.com/locate/brainres

BRAIN RESEARCH

Research Report

Activation of satellite glial cells in lumbar dorsal root ganglia contributes to neuropathic pain after spinal nerve ligation

Feng-Yu Liu[a,1], Yan-Ni Sun[a,1], Fa-Tian Wang[a,1], Qian Li[a], Li Su[a], Zi-Fang Zhao[a], Xiang-Ling Meng[a], Hong Zhao[a], Xi Wu[a], Qian Sun[b], Guo-Gang Xing[a,*], You Wan[a,b,c,*]

[a]Neuroscience Research Institute, Peking University, Beijing 100191, PR China
[b]Department of Neurobiology, School of Basic Medical Sciences, Peking University, Beijing 100191, PR China
[c]Key Laboratory for Neuroscience, the Ministry of Education/the Ministry of Public Health, Peking University, Beijing 100191, PR China

ARTICLE INFO

Article history:
Accepted 10 October 2011
Available online 14 October 2011

Keywords:
Neuropathic pain
Satellite glial cell
Mechanical allodynia
Fluorocitrate
Glial fibrillary acidic protein (GFAP)

ABSTRACT

The role of satellite glial cells (SGCs) of sensory ganglia in chronic pain begins to receive interest. The present study aims to investigate the contribution of SGC activation to the development of neuropathic pain. A neuropathic pain model was established by lumbar 5 spinal nerve ligation (SNL), and glial fibrillary acidic protein (GFAP) was used as a marker of SGC activation. It was found that SGCs were activated in the ipsilateral dorsal root ganglia (DRG) increased significantly as early as 4 h following SNL, gradually increased to a peak level at day 7, and then stayed at a high level to the end of the experiment at day 56. SGC activation in the SNL group was significantly higher than that in the sham group at days 1, 3 and 7 after operation. Immunofluorescent double labeling showed that the activated SGCs encircled large, medium-sized and small neurons. The SGCs surrounded the small and medium-sized neurons were preferentially activated in the early phase, but shifted to large diameter neurons as time went on. Continuous infusion of fluorocitrate, a glial metabolism inhibitor, to the affected DRG via mini-osmotic pump for 7 d significantly alleviated mechanical allodynia at day 7. These results suggest that SGCs in the DRG were activated after SNL. SGC activation contributed to the early maintenance of neuropathic pain.

1. Introduction

Glial cells participate in normal and pathological processes of the central nervous system (CNS) (Allen and Barres, 2009; Benarroch, 2005; De Keyser et al., 2008; Markiewicz and Lukomska, 2006; Miller, 2005). There are strong evidence that CNS glial cells (microglia and astrocytes) implicate in induction and maintenance of neuropathic pain (Cao and Zhang, 2008; Lee et al., 2010; Scholz and Woolf, 2007; Suter et al., 2007; Watkins and Maier, 2002; Zhuang et al., 2006). In

* *Corresponding authors at:* Neuroscience Research Institute, Peking University, 38 Xue-Yuan Road, Beijing 100191, PR China. Fax: +86 10 82805185.
E-mail addresses: ywan@hsc.pku.edu.cn (Y. Wan), ggxing@bjmu.edu.cn (G.-G. Xing).

Abbreviations: CNS, central nervous system; SGCs, satellite glial cells; TNF-α, tumor necrosis factor-α; GFAP, glial fibrillary acidic protein; CCI, chronic constriction injury; SNL, spinal nerve ligation; DRG, dorsal root ganglia; PWT, paw withdrawal threshold; GFAP-ir, GFAP-immunoreactivity; NF200, neurofilament 200; IB4, isolectin B4; CGRP, calcitonin gene-related peptide; AUC, area under the curve; Kir4.1, inward rectifying K^+; MMP-2, matrix metalloproteases-2; IL-1β, interleukin-1beta; PFA, paraformaldehyde; PB, phosphate buffer; PBS, phosphate buffered saline; SDS-PAGE, sodium dodecyl sulfate-polyacrylamide gel electrophore; FC, fluorocitrate

[1] These authors contributed equally to this work.

0006-8993/$ – see front matter © 2011 Elsevier B.V. All rights reserved.
doi:10.1016/j.brainres.2011.10.016

the peripheral nervous system, neurons located in sensory ganglia were tightly surrounded by satellite glial cells (SGCs) (Pannese, 2010). Following injury to a peripheral nerve, SGCs underwent changes in cell number, structure and function, similar to those found in the CNS (Cherkas et al., 2004; Hanani, 2005; Ohara et al., 2009). Peripheral nerve transection increased gap junction and intercellular coupling of SGCs, decreased membrane resistance (Cherkas et al., 2004). SGCs also upregulated the production of proinflammatory cytokines such as tumor necrosis factor-α (TNF-α) after lumbar facet joint injury (Miyagi et al., 2006).

Glial fibrillary acidic protein (GFAP) is a marker of the activated SGCs as well as astrocytes (Takeda et al., 2007). Several reports demonstrated that GFAP expression was upregulated in SGCs after tooth pulp injury (Stephenson and Byers, 1995), upper molar extraction (Gunjigake et al., 2009), nerve transection (Woodham et al., 1989), chronic constriction injury (CCI) (Dubový et al., 2010; Ohara et al., 2008; Vit et al., 2006), partial nerve ligation (Xu et al., 2008a), spared nerve injury and L4 spinal nerve ligation (SNL) (Xie et al., 2009). However, no report has shown the activation of SGCs in dorsal root ganglia (DRG) after L5 SNL in rats, especially much less is known about the possible role of SGCs in neuropathic pain.

In the present study, we investigated whether SGCs were activated after L5 SNL first, then we determined whether the activated SGCs played a role in neuropathic pain. These findings raised the possibility of targeting peripheral SGCs for the treatment of neuropathic pain.

2. Results

2.1. *Development of mechanical allodynia in SNL rats*

After ligation of the left L5 spinal nerve, mechanical allodynia developed in the ipsilateral hind paw. 50% paw withdrawal threshold (PWT) to calibrated *von Frey* filaments gradually decreased as time going on, as shown in Fig. 1. At 12 h, a significant decrease in 50% PWT was observed in SNL rats as compared to that in the sham-operated rats. Up to 56 d after SNL, mechanical allodynia existed continuously.

2.2. *Time course of SGC activation after SNL*

In the SNL group, the time course of the SGC activation was observed. Fig. 2A is an example of immunohistochemical staining of GFAP-immunoreactivity (GFAP-*ir*) in L5 DRG on the pre-operation day (control) and at 4 h, 8 h, 12 h, 1 d, 3 d, 7 d, 14 d, 28 d and 56 d after SNL. The percentages of the GFAP-*ir*-encircled neurons were plotted as shown in Fig. 2B. In control rats, only 16.4%±1.5% of the neurons in the ipsilateral DRG were surrounded by GFAP-*ir* SGCs. As early as 4 h after SNL, the GFAP-*ir* increased (33.5%), then gradually reached to a peak level (92.2%) at day 7 and stayed at a high level throughout the remaining observation period of the experiment to 61.7% at day 14, 61.4% at day 28 and at 75.1% at day 56 (the longest time point examined in the present study).

In the sham-operated rats, the time course of GFAP-*ir* was shown in Fig. 3A. It was observed at 4 h, 8 h, 12 h, 1 d, 3 d, 7 d, 14 d, 28 d and 56 d after operation. Percentage of GFAP-*ir*-encircled neurons was shown in Fig. 3B. It can be seen that the percentage of GFAP-*ir*-encircled neurons also significantly increased from 4 h to 56 d.

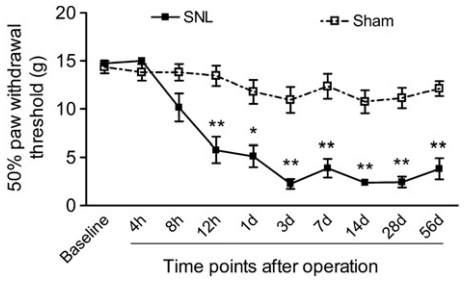

Fig. 1 – Development of mechanical allodynia after SNL. Mechanical allodynia was tested with *von Frey* filament within 56 d after SNL. 50% paw withdrawal threshold (PWT) significantly decreased from 12 h after SNL and continuously existed until 56 d compared to that in the sham-operated group. No obvious allodynia was observed in the sham-operated rats. * $p<0.05$, ** $p<0.01$ compared with the sham-operation group. n=13.

From Figs. 2 and 3, it was easy to see that the number of the GFAP-*ir*-encircled neurons increased in the SNL group and also in the sham-operation group, but the degree of increase in the SNL group was much higher. For example, the highest percentage at day 7 in the SNL group was 92.2%±1.2%, while in the sham-operation group, it was 67.9%±2.2%.

Comparison between the SNL and the sham-operated animals showed that the percentage of neurons encircled by GFAP-*ir* SGCs in the SNL group was significantly higher than that in the sham group at 1 d, 3 d and 7 d after operation (Fig. 3C).

Western blot was performed to analyze GFAP protein expression in DRG. Results at different time points up to 28 d are shown in Fig. 4. A representative result is shown in Fig. 4A. Statistical results showed that GFAP protein expression in L5 DRG increased at different time points after SNL (Fig. 4B) and sham-operation (Fig. 4C). Comparison between the SNL and the sham-operated animals showed that GFAP protein expression in the SNL group was significantly higher than that in the sham group at 3 d, 7 d and 14 d after operation (Fig. 4D).

2.3. *Types of GFAP-ir-encircled neurons*

There are large, medium-sized and small neurons in the DRG. Different types of DRG neurons have different roles in the development of neuropathic pain. Neurofilament 200 (NF200) is a commonly used marker for large DRG neurons, isolectin B4 (IB4) is a marker for the medium-sized and small, non-peptidergic neurons, and calcitonin gene-related peptide (CGRP) is a marker for the medium-sized and small peptidergic neurons. Double labeling results of GFAP-*ir* with NF200, IB4 or CGRP were shown in Fig. 5. The results showed that the activated SGCs enveloped all three types of DRG neurons, and results at day 1 was presented here as an example.

To observe the dynamic profile of the GFAP-*ir*-encircled neurons, the ratio of the GFAP-*ir*-positive neurons with specific cell

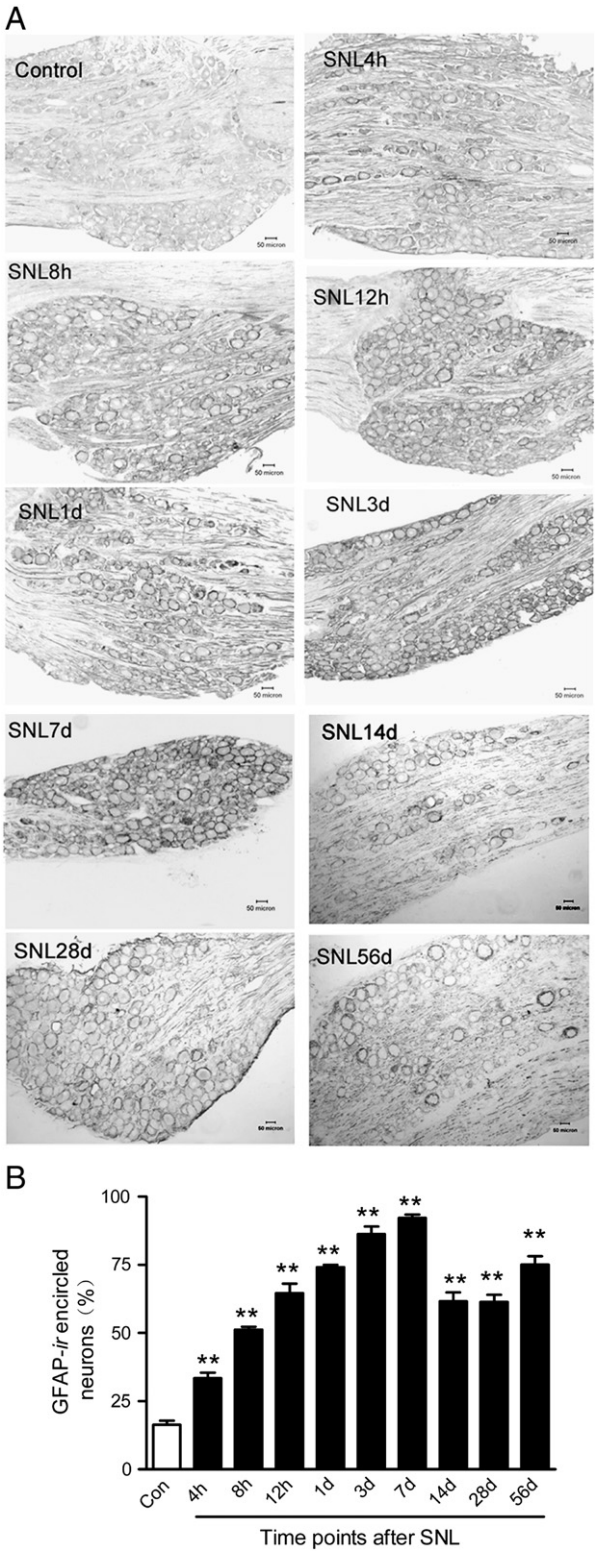

Fig. 2 – Time course of GFAP–*ir* in the L5 DRG after SNL. (A), GFAP-*ir* at 4 h, 8 h, 12 h, 1 d, 3 d, 7 d, 14 d, 28 d and 56 d. Intense GFAP-*ir* was seen around neurons after SNL. Scale bar = 50 μm. (B), Percentage of GFAP-*ir* encircled neurons to the total neurons. Con = control, ** $p < 0.01$ compared with the control. n = 3.

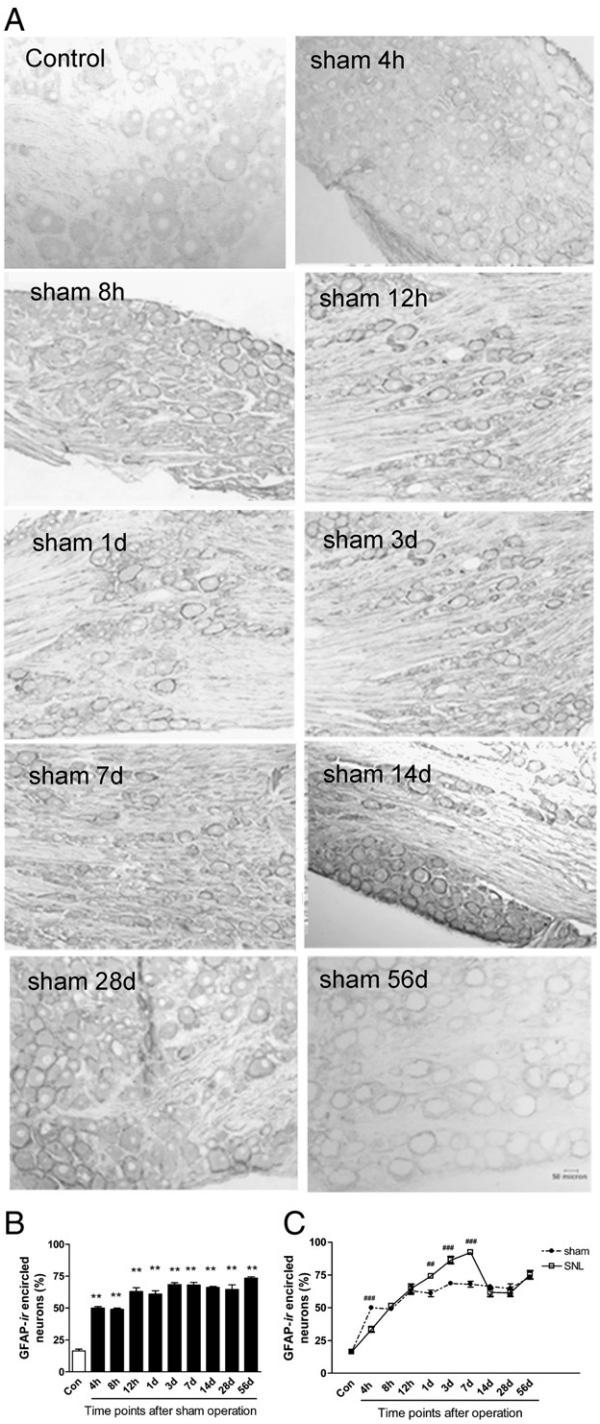

Fig. 3 – Time course of GFAP–*ir* in the L5 DRG following sham operation. (A), GFAP-*ir* at 4 h, 8 h, 12 h, 1 d, 3 d, 7 d, 14 d, 28 d and 56 d. GFAP-*ir* was seen after sham operation. Scale bar = 50 μm. (B), Percentage of GFAP-*ir* encircled neurons to the total neurons. Con = control, ** $p < 0.01$ compared with the control. n = 3. (C), Difference of GFAP-*ir* expression between SNL and sham-operation groups analyzed with two-way ANOVA. The percentage of GFAP-*ir* encircled neurons is significantly higher in the SNL group than that in the sham-operation group at 1 d, 3 d and 7 d after operation. ## $p < 0.01$, ### $p < 0.001$ compared with the sham-operation group.

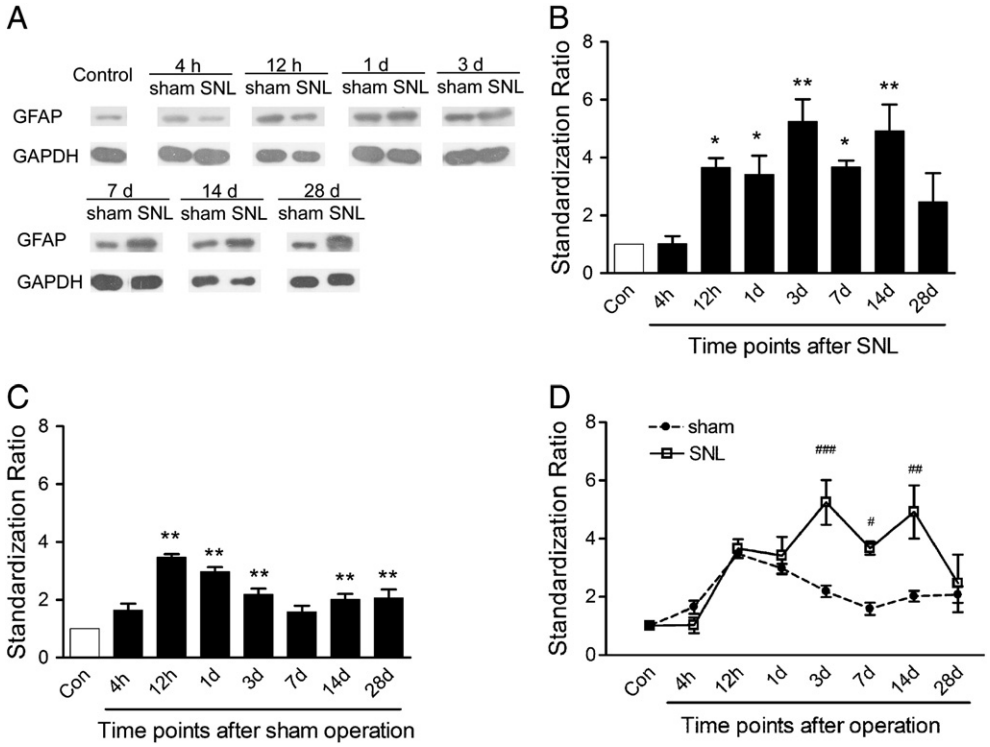

Fig. 4 – Western blot analysis of GFAP protein expression in L5 DRG following SNL and sham operation. (A), Western blot bands at 4 h, 12 h, 1 d, 3 d, 7 d, 14 d and 28 d. (B), Statistical analysis of the ratio between GFAP and GAPDH immunoreactivity in the SNL rats. Con = control, * $p<0.05$, ** $p<0.01$, compared with the control. n=3. (C), Statistical analysis of the ratio between GFAP and GAPDH immunoreactivity in the sham-operated rats. Con = control, ** $p<0.01$, compared with the control. n=3. (D), Two-way ANOVA was used to compare the difference of GFAP protein expression between SNL and sham-operation groups. GFAP protein expression is significantly higher in the SNL group than that in the sham-operation group at 3 d, 7 d and 14 d after operation. $^{\#}$ $p<0.05$, $^{\#\#}$ $p<0.01$, $^{\#\#\#}$ $p<0.001$ compared with the sham-operation group.

area ranges over all GFAP-*ir*-positive neurons was calculated (Fig. 6). The cell areas ranged from 200 to over 4000 μm^2 (equivalent to about 16 to 70 μm of the cell diameters). At different time points after SNL, neurons with different sizes had differential profiles of SGC activation. At 12 h after SNL (Figs. 6A and B), the small and the medium-sized neurons were mainly surrounded with GFAP-*ir* positive staining (activated SGCs); at 7 d, more large neurons were surrounded with the activated SGCs, although there was no statistical difference between 7 d and 12 h ($p=0.16$); at 56 d, more large neurons and less small neurons were encircled by the activated SGCs.

In sham-operated rats, it was found that at different time points (12 h, 7 d and 56 d as examples) after surgery, the distribution pattern of SGCs was similar to that of normal conditions. The activated SGCs wrapped all types of DRG neurons (Figs. 6C and D).

2.4. *Effects of fluorocitrate on mechanical allodynia in SNL rats*

To determine the causal relationship between the SGC activation and neuropathic pain, we further tested if mechanical allodynia could be alleviated when SGC activation was inhibited with fluorocitrate, a glial metabolism inhibitor, perfusion to local L5 DRG. Compared with vehicle, continuous infusion of fluorocitrate to the affected DRG via mini-osmotic pump for 7 d significantly alleviated mechanical allodynia at day 7, but not at day 1 and day 3 (Fig. 7A). At day 14 (7 d after fluorocitrate withdraw), 50% PWTs in the fluorocitrate-treated group did not show any significant difference compared to that in the vehicle-treated group, indicating that the inhibited allodynia returned to pain state. Fig. 7B shows the statistical results with the area under the curve (AUC). Fluorocitrate-treated animals had higher 50% PWTs compared to vehicle-treated ones especially at day 7 ($p<0.01$), suggesting that inhibition of SGC activation alleviated mechanical allodynia.

An additional experiment was performed to evaluate whether fluorocitrate perfused into the L5 DRG could diffuse to the corresponding level of the spinal cord. Alexa Fluor 594, instead of fluorocitrate, was put into the osmotic pump. It is a fluorescent dye with almost same molecular weight to fluorocitrate. In SNL rats, microscopic observation of the DRG in whole-mount showed that Alexa Fluor 594 was steadily observed 7 d in L5 DRG and its dorsal root, but not in the adjacent L4 DRG or spinal cord sections to which these DRG neurons project (data not shown).

2.5. *Effects of fluorocitrate on SGCs and neurons in SNL rats*

At day 7 (when fluorocitrate application was stopped), the SGC activation in the ipsilateral L5 DRG was examined. The GFAP-*ir* expression in the SGCs was indicated by red fluorescence

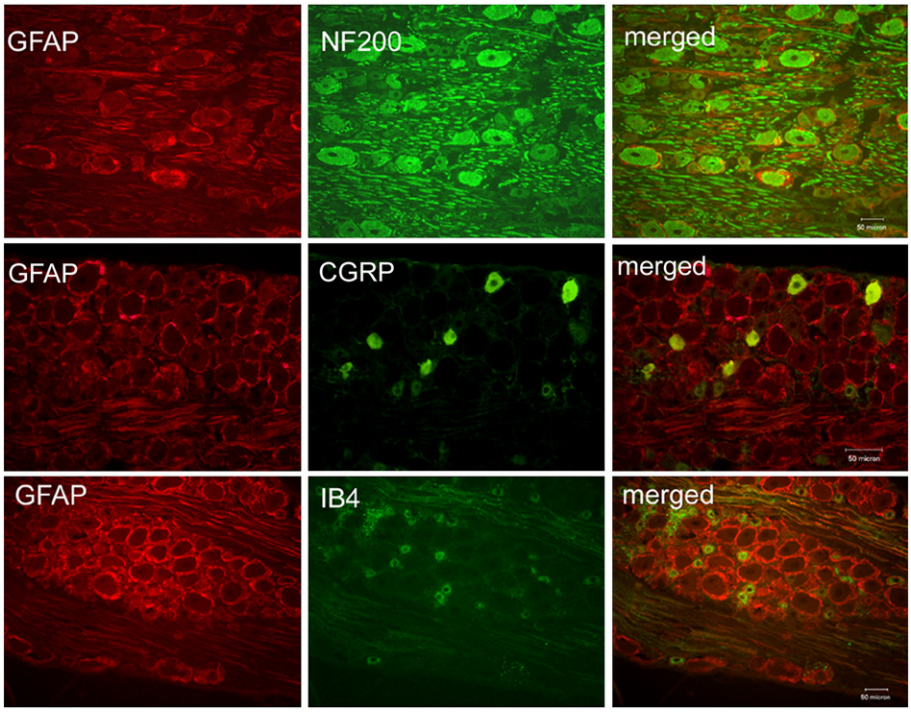

Fig. 5 – An example of immunofluorescent double labeling of GFAP with neuronal markers in L5 DRG after SNL. Distribution of activated SGCs surrounding different types of neurons was tested by double labeling of GFAP (red) with different neuronal markers, NF-200 (green) for large DRG neurons, CGRP (green) and IB4 (green) for small and the medium-sized peptidergic and non-peptidergic neurons. Scale bar=50 μm.

(Figs. 8A–C). After treatment with fluorocitrate for 7 d, the average intensity of GFAP-*ir* staining in the fluorocitrate-treated group decreased compared with that in the vehicle-treated group (14.0±0.7 *vs* 22.0±2.4) ($p<0.01$).

In order to examine whether fluorocitrate damage neurons, we measured the expression of neuron markers (NF200 and CGRP) in the perfused DRG. The NF200-*ir* and CGRP-*ir* expression in the SGCs was indicated by green fluorescence. After treatment with fluorocitrate for 7 d, the average intensity of NF200-*ir* and CGRP-*ir* staining in the fluorocitrate-treated group was similar with that in the vehicle-treated group (20.7 ±2.4 *vs* 25.9±1.8 for NF200; 13.9±2.0 *vs* 18.3±2.2 for CGRP) ($p>0.05$) (Figs. 8D–I).

3. Discussion

3.1. *Activation of SGCs after spinal nerve ligation (SNL)*

Nerve injury has been shown to lead to activation in SGCs characterized by proliferation and hypertrophy, up-regulation of GFAP expression, increased number of gap junction and coupling among SGCs, increased production of various molecules, such as neurotrophins and TNF-α (Hanani, 2005; Ohara et al., 2009; Takeda et al., 2009). In the present study, we used GFAP as a major marker for SGC activation in DRG. GFAP was present at low levels in normal SCGs, making this a particularly useful marker for quantitative and semi-quantitative measurement of SGC activation. Up-regulation of GFAP in SGCs after nerve injury has been reported in other chronic pain models (Dubový et al., 2010; Gunjigake et al., 2009; Ohara et al., 2008; Stephenson and Byers, 1995; Woodham et al., 1989; Xie et al., 2009; Xu et al., 2008a). Association of a particular molecule with SGC activation was essentially defined by using GFAP to measure SGC activation (Miyagi et al., 2006; Ohtori et al., 2004; Takeda et al., 2007; Xu et al., 2006). Hence, GFAP is a most widely used and robust early marker for activation of SGCs.

A systematic and long-term observation of SGC activation in DRG after L5 SNL was carried out for the first time in the present study. By immunohistochemical staining, it was found that the basal level of GFAP expression of SGCs was quite low, only about 16.4% neurons were encircled by GFAP-*ir* SGCs in normal DRG in our experiment, similar to that in previous report (Woodham et al., 1989). After SNL, GFAP-*ir* expression in SGCs increased in the ipsilateral DRG (Fig. 2). This activation occurred as early as 4 h (33.5%) to as late as 56 d (75.1%) after SNL, reached a peak level at 7 d (92.2%). Denser immunohistochemical staining was seen with GFAP-*ir* in the SGCs, suggesting that the activated SGCs likely expressed more GFAP.

We also observed SGC activation in sham-operated rats. However, the activation degree in sham-operated rats was much lower than that in SNL rats, especially at 1 d, 3 d and 7 d. For example, the percentage of GFAP-*ir* encircled neurons in sham-operated rats was 67.9% at day 7, while in SNL rats, it was 92.2% (Fig. 3C).

In the present study, Western blot was performed to examine GFAP protein expression in L5 DRG (Fig. 4). Results

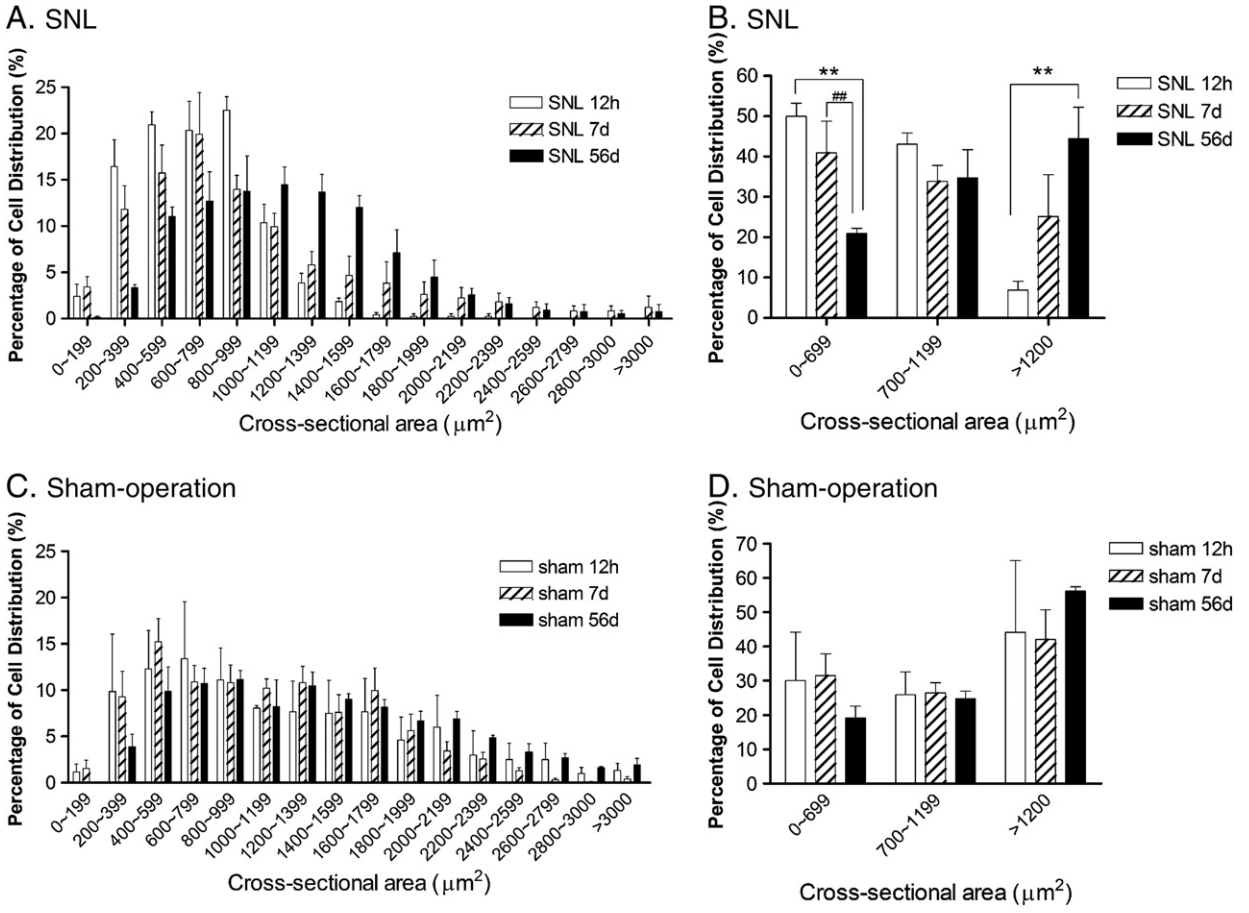

Fig. 6 – Spatiotemporal distribution diagram of DRG neurons encircled by GFAP-*ir* SGCs. Each column represents the ratio of the number of neurons within the given 200-μm² subdivision to the total number of neurons encircled by GFAP-*ir* SGCs at 12 h, 7 d and 56 d in SNL (A) and sham-operation group (C). Each column represents the ratio of the number of small, medium-sized and large neurons to the total number of neurons encircled by GFAP-*ir* SGCs at 12 h, 7 d and 56 d in the SNL (B) and the sham-operation group (D). ** $p<0.01$ compared with the SNL group at 12 h. ## $p<0.01$ compared with the SNL group at 7 d. n=3.

obtained from Western blot almost confirmed those obtained from immunohistochemical staining. For example, GFAP protein expression was all increased relative to control after L5 SNL or sham-operation. What we should notice is that there were some differences between the results of two methods. First, immunohistochemical staining indicated that the SGC activation occurred as early as 4 h after L5 SNL or sham-operation. However, Western blot results showed that GFAP protein expression in L5 DRG did not change at 4 h after L5 SNL or sham-operation. Second, there were some discrepancies in the time courses during which activation degree in SNL group was higher than that in sham-operation group. The time courses were from 1 d to 7 d in immunohistochemical experiments, while the time courses were from 3 d to 14 d in Western blot experiments. The difference may be related to GFAP source in DRG. GFAP originated from the SGCs and the Schwann cells in peripheral DRG. In immunohistochemical experiments, we focused on the GFAP-*ir* SGCs in DRG and calculated the percentage of neurons surrounded with GFAP-*ir* SGCs. In Western blot experiments, GFAP protein originated from SGCs and Schwann cells. Previous study reported that peripheral nerve injury activated Schwann cells and increased the GFAP expression (Kirsch et al., 1998; Xu et al., 2008b). So, for the studies of SGCs activation, immunohistochemistry may be more sensitive than Western blot.

3.2. *Possible role of activated SGCs in L5 DRG in neuropathic pain*

In the present study, we found that the animals developed mechanical allodynia by 12 h after L5 SNL. In the sham-operation group, no mechanical allodynia was observed (Fig. 1).

For the first 3 time points (from 4 h to 12 h) and the last 3 time points (from 14 d to 56 d), SGCs were activated in both SNL and sham-operated rats, and SGC activation in SNL rats was similar with that in sham-operated rats. But only SNL rats developed mechanical allodynia. So, this result may suggest that the activated SGCs did not play a role in the initiation and late maintenance of allodynia after SNL.

From 1 d to 7 d, SGCs were also activated in SNL and sham-operated rats. But SGC activation in SNL group was significantly higher than that in the sham group. SNL rats developed

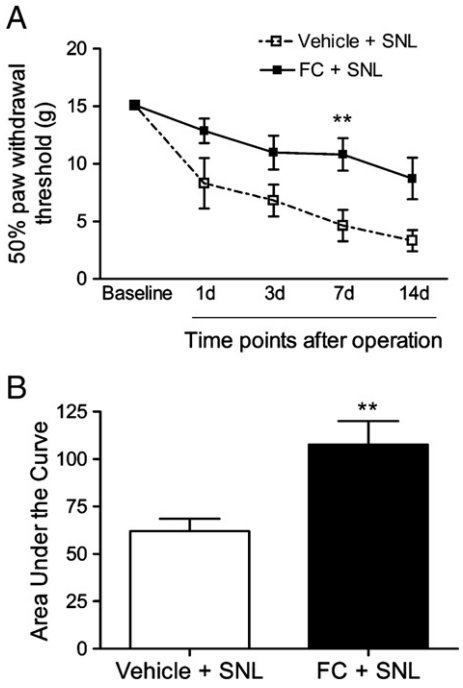

Fig. 7 – Effects of fluorocitrate (FC) application through mini-osmotic pump to DRG on mechanical allodynia. Mechanical allodynia was tested with 50% PWT, 0.084 mmol·L^{-1} fluorocitrate was administrated to inhibit SGC activation for 7 d after SNL. (A), The 50% PWT in the fluorocitrate or vehicle-treated group. ** $p<0.01$ compared with the vehicle-treated group. (B), Statistical analysis with area under the curve (AUC) of the two groups. Significant difference was found between fluorocitrate-treated and vehicle-treated groups with Student's *t*-test ($p<0.01$).**

mechanical allodynia, but sham-operated rats did not. So, the activated SGCs may play a role in the early maintenance of allodynia after SNL.

Furthermore, a glial metabolism inhibitor fluorocitrate was applied to L5 DRG by infusion with mini-osmotic pump. This application aimed to test the causal relationship between the SGC activation and mechanical allodynia. Fluorocitrate selectively inhibits the tricarboxylic acid cycle in astrocytes and microglia by blocking aconitase, a metabolic enzyme just used in glia, other than neurons. Many previous studies have reported that, it is a relatively narrow dose range for fluorocitrate resulting in a reversible inhibition of the metabolism in the glial cells and not destruction of the neurons (Hayakawa et al., 2010; Paulsen et al., 1987). Optimization studies were performed to select the fluorocitrate concentration (0.084 mmol·L^{-1}, flow rate: 1 μL·h^{-1} for 7 d; equal to 2 nmol/d). After fluorocitrate administration to the ipsilateral L5 DRG for 7 d, activation of SGCs (demonstrated by increased GFAP-*ir* expression) decreased, as compared with that in the vehicle-treated group (Figs. 8A–C). At the same time, mechanical allodynia was also inhibited (Fig. 7). On the other hand, fluorocitrate at this concentration did not affect the expression of NF200 and CGRP (Figs. 8D–I). At day 14 (7 d after fluorocitrate withdraw) after SNL, there was a lack of difference in neuropathic pain behavior between the fluorocitrate and the vehicle animals, indicating that the inhibited allodynia returned to pain state. Although SGCs were activated at day 1 and day 3 after SNL, there was a lack of difference in neuropathic pain behavior between the fluorocitrate and the vehicle animals. These findings provided direct evidence that SGC activation contributed to the early maintenance of allodynia after SNL, especially at 7 d.

Concerns have been raised about two likelihoods. First, during the delivery for 7 d, fluorocitrate may diffuse into adjacent DRG, the spinal cord from the perfused DRG, then relieve the mechanical allodynia. Alexa Fluor 594, which has a molecular weight similar to that of fluorocitrate (820 *vs.* 826.16) was put into the osmotic pump. Microscopic observation of the DRG in whole-mount showed that fluorescence was steady in the perfused DRG and its dorsal root, but not in the adjacent DRG or spinal cord. So, the first likelihood seemed unlikely in view of the local perfusion of Alexa Fluor 594. Secondly, the dose of fluorocitrate (0.084 mmol·L^{-1}, flow rate: 1 μL·h^{-1} for 7 d; equal to 2 nmol/d) may result in damage to neurons. In the previous reports, microinjection of fluorocitrate (2 nmol/d) resulted in irreversible degeneration of neurons (Hayakawa et al., 2010; Paulsen et al., 1987). In the present study, fluorocitrate administration (2 nmol/d) for 7 d, inhibited the activation of SGCs (demonstrated by decreased GFAP-*ir* expression), but did not affect neurons (demonstrated by no obvious change of NF200-*ir* and CGRP-*ir* expression). This discrepancy may be related to differences in the route of drug application. For example, in Paulsen's study, one microliter fluorocitrate (1 mmol·L^{-1}, flow rate: 0.25 μl·min^{-1}; equal to 2 nmol/d) was injected continuously by a slow-injection pump, whereas in our experiment, fluorocitrate (0.084 mmol·L^{-1}, flow rate: 1 μL·h^{-1} for 7 d; equal to 2 nmol/d) was infused with mini-osmotic pump. Compared with their studies, the concentration are lower and infusion speed of are more slow in the present studies. The effect of fluorocitrate is mild and long-lasting in the present studies. So, the second likelihood seemed unlikely in view of the application method. We suggest that fluorocitrate (0.084 mmol·L^{-1}, flow rate: 1 μL·h^{-1} for 7 d; equal to 2 nmol/d) infused to L5 DRG in SNL rats with mini-osmotic pump, induces an *in vivo* condition in which the SGCs energy metabolism is selectively impaired, and that this condition could be used as a model for study of the relationships between neurons and SGCs and the importance of SGCs for neuropathic pain *in vivo*.

Under normal conditions, SGCs mainly locate in a dispersed manner in all types of DRG neurons (Fig. 2, Control). In the sham-operation rats, at different time points (12 h, 7 d and 56 d) after surgery, the distribution pattern of SGCs was similar to that under normal conditions, *i.e.*, the activated SGCs wrapped all types of DRG neurons (Figs. 6C and D). In SNL rats, the distribution pattern changed dramatically at different time points (Figs. 6A and B). Activated SGCs surrounded small to the medium-sized neurons at 12 h after SNL. As time passed, there was a shift of GFAP-*ir* SGCs distribution from small to large ones. The activated SGCs seemingly wrapped more large DRG neurons at day 7, and wrapped more large neurons at day 56. It is well known that large Aβ-fiber DRG neurons participated in mechanical allodynia in SNL rats (Song et al., 2003; Xie et al., 2005). Previous reports have shown that the number of small neurons decreased

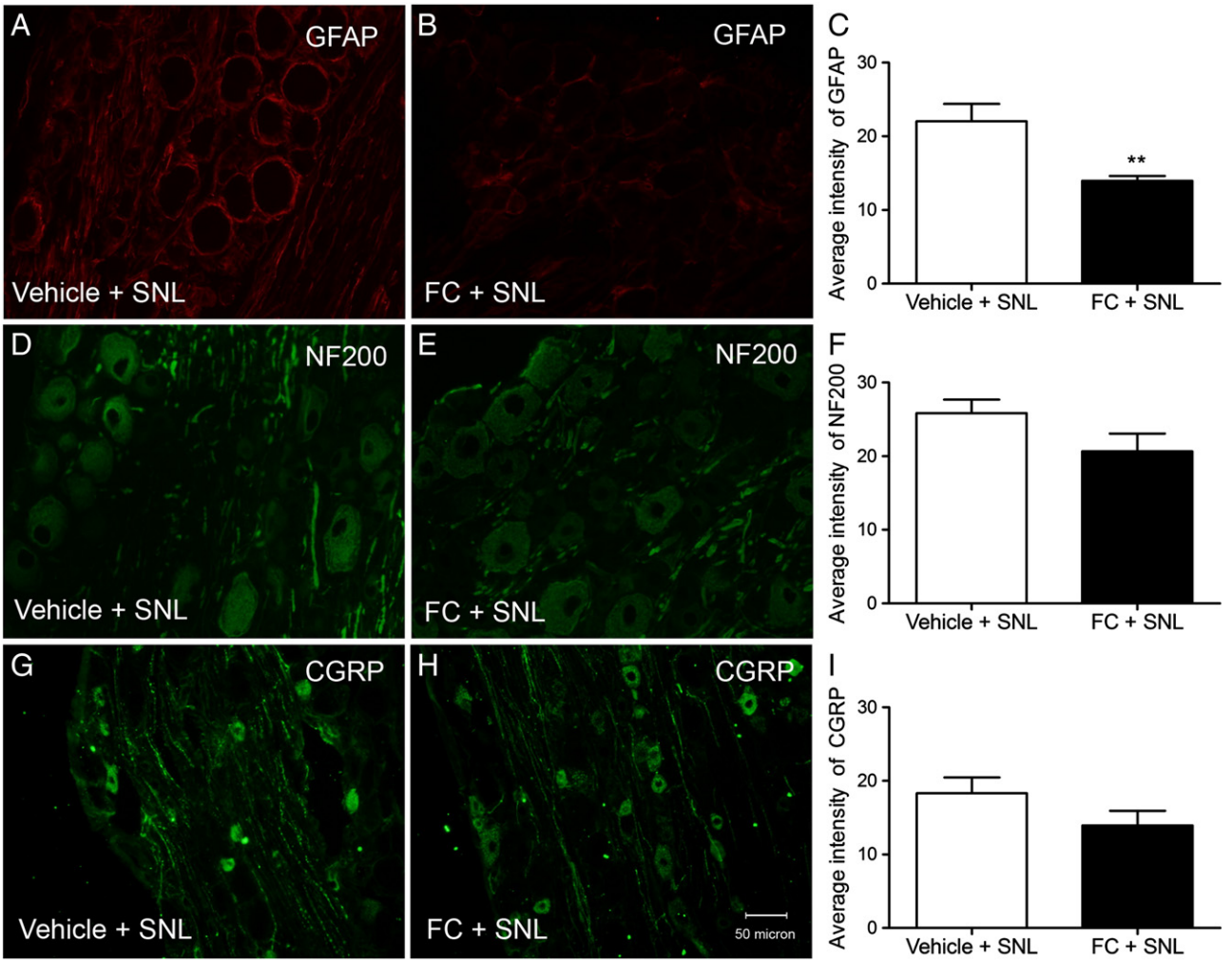

Fig. 8 – Effects of fluorocitrate (FC) on GFAP-*ir*, NF200-*ir* and CGRP-*ir* expression at day 7 in SNL rats. GFAP-*ir* of SGCs was labeled as red fluorescence. NF200-*ir* and CGRP-*ir* of SGCs was labeled as green fluorescence. Fluorocitrate or vehicle was applied through osmotic pump after SNL same as in Fig. 7. (A), GFAP-*ir* expression in vehicle-treated group. (B) GFAP-*ir* expression in fluorocitrate group. (C), Statistical analysis GFAP-*ir* expression of the two groups. (D), NF200-*ir* expression in vehicle-treated group. (E) NF200-*ir* expression in fluorocitrate group. (F), Statistical analysis NF200-*ir* expression of the two groups. (G), CGRP-*ir* expression in vehicle-treated group. (H) CGRP-*ir* expression in fluorocitrate group. (I), Statistical analysis CGRP-*ir* expression of the two groups. ** $p<0.01$ compared with the vehicle-treated group. Scale bar=50 μm. n=5 in fluorocitrate group; n=4 in vehicle-treated group.

after axotomy (Tandrup et al., 2000), which may partially contribute to this phenomenon. Our results provide another possible mechanism underlying participation of large DRG neurons in mechanical allodynia.

How activated SGCs participated in neuropathic pain was of great interest and may open a range of new possibilities for neuropathic pain treatment (Jasmin et al., 2010). Recent studies have demonstrated that SGCs were able to modulate neuronal excitability, then lead to neuropathic pain (Hanani, 2005; Takeda et al., 2009). Potassium ion channels expressed by SGCs regulated the extracellular K^+ concentration, which determined the neuronal excitability. It has been shown that glia-specific inward rectifying K^+ ($K_{ir}4.1$) channels in SGCs were reduced after CCI of the infraorbital nerve, resulting in a decrease of K^+ buffering capacity of SGCs, an increase in extracellular K^+ concentration and augmented excitability of neurons (Vit et al., 2006, 2008). Reduction of the $K_{ir}4.1$ channel in SGCs was sufficient to produce neuropathic pain-like behavior in rats. In addition, coupling between adjacent SGCs via gap junctions regulated perineuronal environment. Following peripheral nerve injury, there was a great increase in gap junction-mediated coupling among SGCs (Cherkas et al., 2004; Hanani et al., 2002), consistent with an up-regulation of the gap junction protein connexin 43 and a decrease in membrane resistance (Ohara et al., 2008; Pannese et al., 2003). Augmented coupling may facilitate communication between neurons by increasing the passage of

electric current and/or movement of nociceptive-related signaling molecules such as ATP and cyclic nucleotides (Ohara et al., 2008). Gap junction blockers abolished the inflammation-induced changes in SGCs and neurons (Dublin and Hanani, 2007; Huang et al., 2010).

Previous studies suggested that chemokine signaling has emerged as a key candidate to mediate glia–neuron interaction. SGCs upregulated the production of proinflammatory cytokines such as TNF-α after peripheral nerve injury (Miyagi et al., 2006). The increased expression of TNF-α in SGCs and the expression of p55 in the neurons encircled by SGCs indicated that activation of SGCs may increase the neuronal excitability via a TNF-α paracrine mechanism. More recently, it has been reported that SNL induced persistent up-regulation of matrix metalloproteases-2 (MMP-2) in SGC of the L5 DRG, which maintained neuropathic pain via interleukin-1beta (IL-1β) cleavage in the DRG (Dev et al., 2010; Ji et al., 2009; Kawasaki et al., 2008). SGCs in the trigeminal ganglia could enhance the neuronal excitability through IL-1β in inflammatory pain models (Takeda et al., 2007).

3.3. *The possible mechanisms of SGC activation*

Recently, the mechanism by which peripheral nerve injury causes activation of SGCs has begun to attract attention. One possibility was abnormal spontaneous activity in the sensory neurons. First, blocking spontaneous activity with TTX, bupivacaine or lidocaine prevented the activation of the glial cells in the DRG and the spinal cord in chronic pain models (Guo et al., 2007; Ren and Dubner, 2008; Wen et al., 2007; Xie et al., 2009). Secondly, activation of the SGCs after peripheral nerve injury or inflammation has been reported in several different models (Chudler et al., 1997; Stephenson and Byers, 1995; Woodham et al., 1989; Xie et al., 2009; Xu et al., 2008a). Although the time course and degree of SGC activation were not similar in different neuropathic pain models, they were consistent with abnormal spontaneous activity (Chudler et al., 1997; Xie et al., 2009).

In our previous study, we have recorded the spontaneous activity of L5 dorsal root in L5 SNL and sham-operated rats (Sun et al., 2005). Further experiments may be needed to investigate whether spontaneous discharges in SNL and sham groups induce SGC activation.

In conclusion, SGCs in DRG were activated after L5 SNL from a very early time point (4 h) and remained activated for up to at least 56 d. SGC activation in the SNL group was significantly higher than that in the sham group at 1 d, 3 d and 7 d after operation. The application of fluorocitrate into L5 DRG significantly alleviated mechanical allodynia, especially at 7 d. These findings suggested that SGC activation contributed to the early maintenance of allodynia after SNL, especially at 7 d. The present study raised a possibility of targeting SGCs for the treatment of neuropathic pain.

4. Experimental procedure

4.1. *Experimental animals*

Male Sprague–Dawley rats weighing 180–220 g were provided by the Department of Experimental Animal Sciences, Peking University Health Science Center and were habituated to the testing paradigms for 7 d before data collection. Animals had free access to food and water during experiments and were maintained on natural diurnal cycles. All protocols were approved by the Animal Use and Care Committee of our university. Measures were taken to minimize the animals' discomfort, and all experiments adhered to the Guidelines of the Committee for Research and Ethical Issues of the IASP (Zimmermann, 1983).

4.2. *Spinal nerve ligation (SNL)*

Ligation of the left L5 spinal nerve was performed as described by Kim and Chung (Kim and Chung, 1992). Rats were anesthetized with chloral hydrate (0.3 mL/100 g, *i.p.*). An incision was made at the left side of the spine at the L4–S2 level. The L5 transverse process was removed to expose the L5 spinal nerve. The L5 spinal nerve was isolated carefully and ligated tightly with 6–0 silk thread 5–10 mm distal to the L5 DRG. The animals in the sham operation group received the same operation except for ligation of the nerve. Penicillin was used for infection prophylaxis after surgery.

4.3. *Behavioral test*

Behavioral evaluation was done blindly with respect to the condition of the rats (SNL *vs.* sham-operation). Mechanical sensitivity of the left hind paw was tested before and 4 h–56 d after SNL. The 50% PWT in response to a series of *von Frey* filaments was determined by the up-down method (Chaplan et al., 1994) as in our previous report (Jiang et al., 2008; Liu et al., 2010, 2011; Sun et al., 2005; Tong et al., 2010; Xing et al., 2007). Briefly, the rat was placed on a metal mesh floor covered with an inverted clear plastic cage (18×8×8 cm) and allowed a 15-min period for habituation. Eight *von Frey* filaments with approximately equal logarithmic incremental (0.224) bending forces were chosen (0.41, 0.70, 1.20, 2.00, 3.63, 5.50, 8.50, and 15.10 g). Each trial started with a *von Frey* force of 2.00 g delivered perpendicularly to the plantar surface of the left hind-paw. An abrupt withdrawal of the foot during stimulation or immediately after the removal of the filament was recorded as a positive response. Once a positive or negative response was evoked, the next weaker or stronger filament was applied. This procedure was repeated until 6 stimuli after the first change in response had been observed. The 50% PWT was calculated using the following formula: $50\%\ \mathrm{PWT} = 10^{(X+kd)}/10^4$, where X is the value of the final *von Frey* filament used (in log units), k is a value measured from the pattern of positive/negative responses, and d=0.224 which is the average interval (in log units) between the *von Frey* filaments (Dixon, 1980). If an animal responded to the lowest *von Frey* filament, a value of 0.25 g was assigned; if an animal did not respond to the highest *von Frey* filament, the value was recorded as 15.0 g.

4.4. *Immunohistochemistry*

At time points of 4 h, 8 h, 12 h, 1 d, 3 d, 7 d, 14 d, 28 d and 56 d after surgery (n=3 for each time point), the rats were anesthetized with chloral hydrate and perfused through the aorta with 200 mL of normal saline (0.9% NaCl), followed by 300 mL of 4% paraformaldehyde (PFA, pH 7.4) in 0.1 $\mathrm{mol \cdot L^{-1}}$

phosphate buffer (PB, pH 7.4). The L5 DRG was removed, and post-fixed in PFA for 4–6 h, and then cryoprotected in ascending graded sucrose solutions overnight. The DRG was then cut into 8-μm-thick serial sections with a cryostat (Cryocut 1800; Leica Instruments) and mounted on gelatin/chrome alum-coated glass slides.

Immunohistochemistry was performed as in our previous reports (Jiang et al., 2008; Luo et al., 2004; Tu et al., 2004; Yu et al., 2008). Sections were blocked with 2% normal goat serum for 30 min at 37 °C, and then incubated overnight at 4 °C in a humid chamber with primary polyclonal antibody GFAP (rabbit anti-rat, 1:750; Dako), and diluted in phosphate buffered saline (PBS) containing 0.3% Triton X-100 and 1% bovine serum albumin. After washing in 0.01 mol·L^{-1} PBS, sections were incubated with biotinylated secondary antibody to rabbit IgG, followed by incubation with streptavidin-conjugated horseradish peroxidase for 30 min. Sections were then washed in PBS and processed with chromogen (diaminobenzidine, 1 mg/mL; ammonium nickel sulfate, 80 mg/mL; 0.001% H_2O_2).

For immunofluorescent double labeling, DRG sections were incubated overnight at 4 °C with a mixture of rabbit anti-rat GFAP antibody (1:200; Dako), goat anti-rat NF200 (1:2000; Sigma), IB4-FITC (10 μg/mL; Sigma) or goat anti-rat CGRP (1:1000; Sigma). After washing with PBS, the sections were incubated with a mixture of TRITC- or FITC-conjugated secondary antibodies for 1 h at room temperature (for TRITC, 1:100 Sigma; for FITC, 1:100; Sigma). The stained sections were viewed and photographs were taken with a fluorescent microscope (DMIRB; Leica).

4.5. *Western blot detection of GFAP protein expression*

Western blot was used to analyze the changes in GFAP protein expression. According to the immunohistochemical staining of GFAP in L5 DRG on control and at different time points after operation, only time points of 4 h, 12 h, 1 d, 3 d, 7 d, 14 d and 28 d were chosen (n = 3 for each time point). Western blot was performed as described in our previous report (Jiang et al., 2008; Yu et al., 2008). Briefly, animals were decapitated under anesthesia with an over-dose of chloral hydrate. The left L5 DRG was removed, quickly frozen in liquid nitrogen and stored at −80 °C. Frozen tissues were homogenized in homogenization buffer (50 mmol·L^{-1} Tris·base, 2 mmol·L^{-1} EDTA, 40 mmol·L^{-1} NaF, 1 mmol·L^{-1} phenylmethylsulfonyl fluoride). Protein concentration was quantified by the method of BCA protein assay (Redinbaugh and Turley, 1986; Smith et al., 1985). Each sample containing 20 μg of protein was mixed with one fifth volume of 5× loading buffer and heated to 100 °C for 5 min. Protein samples were separated by sodium dodecyl sulfate-polyacrylamide gel electrophoresis (SDS-PAGE, 10%) and transferred to PVDF film. The blots were blocked with 5% non-fat milk for 1 h and incubated with polyclonal rabbit anti-GFAP antibody (1:10000, Dako) and with monoclonal GAPDH (1:8000, Sigma) as loading control overnight at 4 °C. The blots were then incubated for 1 h at room temperature with HRP-conjugated goat anti-rabbit IgG or HRP-conjugated goat anti-mouse IgG secondary antibody (1:2000, Santa Cruz), developed in chemiluminescence reagents for 1 min and exposed to X-ray sensitive film. The intensity of the blots was quantified with densitometry. For quantification of Western blot signals, the density of bands (GFAP and GAPDH) was measured with the Quantity One Analysis System (Bio-Rad).

4.6. *Mini-osmotic pump implantation into DRG and fluorocitrate application*

The dose of fluorocitrate was chosen according to our preliminary data and to previous reports (Gao and Ji, 2010; Hayakawa et al., 2010; Paulsen et al., 1987; Sun et al., 2009). Fluorocitrate (Sigma) at 0.084 mmol·L^{-1} was prepared following the method of Paulsen et al. (1987), and the pH of the solution was adjusted to 7.4. Vehicle was prepared with identical procedure except for addition the fluorocitrate. A mini-osmotic pump (Alzet® 2001) was connected with PE50 (O.D. 0.965 mm, I.D. 0.58 mm) and PE10 (O.D. 0.61 mm, I.D. 0.28 mm) polyethylene tubing in succession. All mini-osmotic pumps were incubated in sterile saline overnight at 37 °C. The front piece of PE10 was pulled in advance so that the tip of the tube was reduced to a diameter of about 150 μm (Zhou et al., 1999). Totally 12 mini-osmotic pumps were filled with fluorocitrate (0.084 mmol·L^{-1}, flow rate: 1 μL·h^{-1} for 7 d) and 9 pumps with vehicle. The L5 spinal nerve was exposed as described above, the fine tip of the catheter was inserted into the L5 spinal nerve and threaded toward to the L5 DRG (Zhuang et al., 2006). The catheter was immobilized *in situ* by tying it up together with the nerve. The nerve distal to the ligature site was also ligated, the catheter was fixed again by a suture in the adjacent muscle. After such connection, the mini-osmotic pump was planted subcutaneously under the skin of the back. Finally, the incision was sutured.

Mechanical allodynia was tested with *von Frey* filaments as described above on day 1 before mini-osmotic pump implantation, and 1 d, 3 d, 7 d and 14 d after pump implantation. An investigator other than the one who carried out the pump implantation performed the behavior tests blindly.

At day 7 after pump implantation, 7 rats from fluorocitrate group and 4 rats from vehicle-treated group were selected randomly and sacrificed. In order to evaluate the effects of fluorocitrate on SGCs and neurons, GFAP, NF-200 and CGRP expression was evaluated in the ipsilateral L5 DRG of fluorocitrate or vehicle-treated groups (n = 5 in fluorocitrate group; n = 4 in vehicle-treated group). For the remaining rats, the pumps were withdrawn carefully from the body under anesthesia by chloral hydrate. Mechanical allodynia was tested again at day 14 (1 week after pump withdrawal).

In control experiments to determine the likelihood of fluorocitrate diffusing into the spinal cord from the perfused DRG, fluorocitrate was replaced with Alexa Fluor 594 (Invitrogen), which has a molecular weight similar to that of fluorocitrate (820 *vs.* 826.16). For these experiments, Alexa Fluor 594 in DRG and dorsal root was examined with a whole mount DRG preparation and spinal cord sections were prepared from fresh tissue without fixation to avoid possible washing out of Alexa Fluor 594 (Xie et al., 2007, 2009).

4.7. *Image analysis*

The percentage of neurons surrounded with GFAP-*ir* SGCs was calculated at each time point from 4 h to 56 d from

immunohistochemically stained slides as described in our previous report (Luo et al., 2004; Yu et al., 2008). This was done in a blinded manner. Three sections were selected for each DRG with an intervening space of at least 20 μm to avoid a neuron being counted twice. Only those neurons with visible nuclei were counted. A neuron was counted as positive if more than half of its circumference was encircled by GFAP-*ir* SGCs. Ratio of the GFAP-*ir* encircled neurons over the total number of neuronal profiles was calculated in each DRG and then averaged for three ganglia at each time point.

Cross-sectional area distribution in positive (GFAP-*ir* SGC surrounded) neurons was calculated both in the SNL group (time points of 12 h, 7 d and 56 d) and in the sham-operation group. DRG neurons were classified as small (<700 μm^2), medium-sized (700–1200 μm^2) and large (>1200 μm^2) according to the measured cross-sectional area (Novakovic et al., 1998). Only those neurons with visible nuclei were chosen for measurement of their cell area.

For analysis of GFAP, NF-200 and CGRP expression in the ipsilateral L5 DRG of fluorocitrate or vehicle-treated groups, 5 fields of each section at the same magnification were chosen randomly to calculate the average gray intensity value. The average intensity was defined as the difference of the average gray intensity value of a chosen field and the background (Luo et al., 2004).

4.8. *Statistical analysis*

Data are expressed as mean±SEM. Difference between two groups at different time points was analyzed with two-way ANOVA, and differences among different time points were analyzed with one-way ANOVA followed by Dunnett's *post-hoc* test. The Student's *t*-test was used if only two groups were applied. Values of $p<0.05$ were taken to be statistically significant.

Acknowledgments

This work was supported by the grants from National Natural Science Foundation of China (30600173, 81070893, 81171042), "111" Project of the Ministry of Education of China, "973" program of the Ministry of Science and Technology of China (2007CB512501), the Key Project of Chinese Ministry of Education (109003). Authors would like to thank Prof. Michael A. McNutt in the Department of Pathology, School of Basic Medical Sciences, Peking University for his help in the preparation of this manuscript. We would like to thank Dr. Xin-Fu Zhou from Flinders University, Australia for technical support of the mini-osmotic pump application. We also would like to thank Prof. Jun-Ming Zhang and Dr. Wen-Rui Xie from University of Cincinnati, USA for technical support of detecting the fluorescence of Alexa Fluor 594 with a whole-mount DRG and spinal cord sections.

REFERENCES

Allen, N.J., Barres, B.A., 2009. Glia — more than just brain glue. Nature 457, 675–677.

Benarroch, E.E., 2005. Neuron–astrocyte interactions: partnership for normal function and disease in the central nervous system. Mayo Clin. Proc. 80, 1326–1338.

Cao, H., Zhang, Y.Q., 2008. Spinal glial activation contributes to pathological pain states. Neurosci. Biobehav. Rev. 32, 972–983.

Chaplan, S.R., Bach, F.W., Pogrel, J.W., Chung, J.M., Yaksh, T.L., 1994. Quantitative assessment of tactile allodynia in the rat paw. J. Neurosci. Methods 53, 55–63.

Cherkas, P.S., Huang, T.Y., Pannicke, T., Tal, M., Reichenbach, A., Hanani, M., 2004. The effects of axotomy on neurons and satellite glial cells in mouse trigeminal ganglion. Pain 110, 290–298.

Chudler, E.H., Anderson, L.C., Byers, M.R., 1997. Trigeminal ganglion neuronal activity and glial fibrillary acidic protein immunoreactivity after inferior alveolar nerve crush in the adult rat. Pain 73, 141–149.

De Keyser, J., Mostert, J.P., Koch, M.W., 2008. Dysfunctional astrocytes as key players in the pathogenesis of central nervous system disorders. J. Neurol. Sci. 267, 3–16.

Dev, R., Srivastava, P.K., Iyer, J.P., Dastidar, S.G., Ray, A., 2010. Therapeutic potential of matrix metalloprotease inhibitors in neuropathic pain. Expert Opin. Investig. Drugs 19, 455–468.

Dixon, W.J., 1980. Efficient analysis of experimental observations. Annu. Rev. Pharmacol. Toxicol. 20, 441–462.

Dublin, P., Hanani, M., 2007. Satellite glial cells in sensory ganglia: their possible contribution to inflammatory pain. Brain Behav. Immun. 21, 592–598.

Dubový, P., Klusáková, I., Svízenská, I., Brázda, V., 2010. Satellite glial cells express IL-6 and corresponding signal-transducing receptors in the dorsal root ganglia of rat neuropathic pain model. Neuron Glia Biol. 6, 73–83.

Gao, Y.J., Ji, R.R., 2010. Light touch induces ERK activation in superficial dorsal horn neurons after inflammation: involvement of spinal astrocytes and JNK signaling in touch-evoked central sensitization and mechanical allodynia. J. Neurochem. 115, 505–514.

Gunjigake, K.K., Goto, T., Nakao, K., Kobayashi, S., Yamaguchi, K., 2009. Activation of satellite glial cells in rat trigeminal ganglion after upper molar extraction. Acta Histochem. Cytochem. 42, 143–149.

Guo, W., Wang, H., Watanabe, M., Shimizu, K., Zou, S., LaGraize, S.C., Wei, F., Dubner, R., Ren, K., 2007. Glial–cytokine–neuronal interactions underlying the mechanisms of persistent pain. J. Neurosci. 27, 6006–6018.

Hanani, M., 2005. Satellite glial cells in sensory ganglia: from form to function. Brain Res. Rev. 48, 457–476.

Hanani, M., Huang, T.Y., Cherkas, P.S., Ledda, M., Pannese, E., 2002. Glial cell plasticity in sensory ganglia induced by nerve damage. Neuroscience 114, 279–283.

Hayakawa, K., Nakano, T., Irie, K., Higuchi, S., Fujioka, M., Orito, K., Iwasaki, K., Jin, G., Lo, E.H., Mishima, K., Fujiwara, M., 2010. Inhibition of reactive astrocytes with fluorocitrate retards neurovascular remodeling and recovery after focal cerebral ischemia in mice. J. Cereb. Blood Flow Metab. 30, 871–882.

Huang, T.Y., Belzer, V., Hanani, M., 2010. Gap junctions in dorsal root ganglia: possible contribution to visceral pain. Eur. J. Pain 14, 49.e1–49.e11.

Jasmin, L., Vit, J.P., Bhargava, A., Ohara, P.T., 2010. Can satellite glial cells be therapeutic targets for pain control? Neuron Glia Biol. 6, 63–71.

Ji, R.R., Xu, Z.Z., Wang, X., Lo, E.H., 2009. Matrix metalloprotease regulation of neuropathic pain. Trends Pharmacol. Sci. 30, 336–340.

Jiang, Y.Q., Xing, G.G., Wang, S.L., Tu, H.Y., Chi, Y.N., Li, J., Liu, F.Y., Han, J.S., Wan, Y., 2008. Axonal accumulation of hyperpolarization-activated cyclic nucleotide-gated cation channels contributes to mechanical allodynia after peripheral nerve injury in rat. Pain 137, 495–506.

Kawasaki, Y., Xu, Z.Z., Wang, X., Park, J.Y., Zhuang, Z.Y., Tan, P.H., Gao, Y.J., Roy, K., Corfas, G., Lo, E.H., Ji, R.R., 2008. Distinct roles of matrix metalloproteases in the early- and late-phase development of neuropathic pain. Nat. Med. 14, 331–336.

Kim, S.H., Chung, J.M., 1992. An experimental model for peripheral neuropathy produced by segmental spinal nerve ligation in the rat. Pain 50, 355–363.

Kirsch, M., Schneider, T., Lee, M.Y., Hofmann, H.D., 1998. Lesion-induced changes in the expression of ciliary neurotrophic factor and its receptor in rat optic nerve. Glia 23, 239–248.

Lee, S., Zhao, Y.Q., Ribeiro-da-Silva, A., Zhang, J., 2010. Distinctive response of CNS glial cells in oro-facial pain associated with injury, infection and inflammation. Mol. Pain 6, 79.

Liu, F.Y., Qu, X.X., Cai, J., Wang, F.T., Xing, G.G., Wan, Y., 2011. Electrophysiological properties of spinal wide dynamic range neurons in neuropathic pain rats following spinal nerve ligation. Neurosci. Bull. 27, 1–8.

Liu, F.Y., Qu, X.X., Ding, X., Cai, J., Jiang, H., Wan, Y., Han, J.S., Xing, G.G., 2010. Decrease in the descending inhibitory 5-HT system in rats with spinal nerve ligation. Brain Res. 1330, 45–60.

Luo, H., Cheng, J., Han, J.S., Wan, Y., 2004. Change of vanilloid receptor 1 expression in dorsal root ganglion and spinal dorsal horn during inflammatory nociception induced by complete Freund's adjuvant in rats. Neuroreport 15, 655–658.

Markiewicz, I., Lukomska, B., 2006. The role of astrocytes in the physiology and pathology of the central nervous system. Acta Neurobiol. Exp. (Wars.) 66, 343–358.

Miller, G., 2005. The dark side of glia. Science 308, 778–781.

Miyagi, M., Ohtori, S., Ishikawa, T., Aoki, Y., Ozawa, T., Doya, H., Saito, T., Moriya, H., Takahashi, K., 2006. Up-regulation of TNFalpha in DRG satellite cells following lumbar facet joint injury in rats. Eur. Spine J. 15, 953–958.

Novakovic, S.D., Tzoumaka, E., McGivern, J.G., Haraguchi, M., Sangameswaran, L., Gogas, K.R., Eglen, R.M., Hunter, J.C., 1998. Distribution of the tetrodotoxin-resistant sodium channel PN3 in rat sensory neurons in normal and neuro-pathic conditions. J. Neurosci. 18, 2174–2187.

Ohara, P.T., Vit, J.P., Bhargava, A., Jasmin, L., 2008. Evidence for a role of connexin 43 in trigeminal pain using RNA interference in vivo. J. Neurophysiol. 100, 3064–3073.

Ohara, P.T., Vit, J.P., Bhargava, A., Romero, M., Sundberg, C., Charles, A.C., Jasmin, L., 2009. Gliopathic pain: when satellite glial cells go bad. Neuroscientist 15, 450–463.

Ohtori, S., Takahashi, K., Moriya, H., Myers, R.R., 2004. TNF-alpha and TNF-alpha receptor type 1 upregulation in glia and neurons after peripheral nerve injury: studies in murine DRG and spinal cord. Spine 29, 1082–1088.

Pannese, E., 2010. The structure of the perineuronal sheath of satellite glial cells (SGCs) in sensory ganglia. Neuron Glia Biol. 6, 3–10.

Pannese, E., Ledda, M., Cherkas, P.S., Huang, T.Y., Hanani, M., 2003. Satellite cell reactions to axon injury of sensory ganglion neurons: increase in number of gap junctions and formation of bridges connecting previously separate perineuronal sheaths. Anat. Embryol. (Berl.) 206, 337–347.

Paulsen, R.E., Contestabile, A., Villani, L., Fonnum, F., 1987. An in vivo model for studying function of brain tissue temporarily devoid of glial cell metabolism: the use of fluorocitrate. J. Neurochem. 48, 1377–1385.

Redinbaugh, M.G., Turley, R.B., 1986. Adaptation of the bicinchoninic acid protein assay for use with microtiter plates and sucrose gradient fractions. Anal. Biochem. 153, 267–271.

Ren, K., Dubner, R., 2008. Neuron–glia crosstalk gets serious: role in pain hypersensitivity. Curr. Opin. Anaesthesiol. 21, 570–579.

Scholz, J., Woolf, C.J., 2007. The neuropathic pain triad: neurons, immune cells and glia. Nat. Neurosci. 10, 1361–1368.

Smith, P.K., Krohn, R.I., Hermanson, G.T., Mallia, A.K., Gartner, F.H., Provenzano, M.D., Fujimoto, E.K., Goeke, N.M., Olson, B.J., Klenk, D.C., 1985. Measurement of protein using bicinchoninic acid. Anal. Biochem. 150, 76–85.

Song, X.J., Zhang, J.M., Hu, S., Lamotte, R.H., 2003. Somata of nerve-injured sensory neurons exhibit enhanced responses to inflammatory mediators. Pain 104, 701–709.

Stephenson, J.L., Byers, M.R., 1995. GFAP immunoreactivity in trigeminal ganglion satellite cells after tooth injury in rats. Exp. Neurol. 131, 11–22.

Sun, Q., Tu, H., Xing, G.G., Han, J.S., Wan, Y., 2005. Ectopic discharges from injured nerve fibers are highly correlated with tactile allodynia only in early, but not late, stage in rats with spinal nerve ligation. Exp. Neurol. 191, 128–136.

Sun, X.C., Chen, W.N., Li, S.Q., Cai, J.S., Li, W.B., Xian, X.H., Hu, Y.Y., Zhang, M., Li, Q.J., 2009. Fluorocitrate, an inhibitor of glial metabolism, inhibits the up-regulation of NOS expression, activity and NO production in the spinal cord induced by formalin test in rats. Neurochem. Res. 34, 351–359.

Suter, M., Wen, Y.R., Decosterd, I., Ji, R.R., 2007. Do glial cells control pain? Neuron Glia Biol. 3, 255–268.

Takeda, M., Takahashi, M., Matsumoto, S., 2009. Contribution of the activation of satellite glia in sensory ganglia to pathological pain. Neurosci. Biobehav. Rev. 33, 784–792.

Takeda, M., Tanimoto, T., Kadoi, J., Nasu, M., Takahashi, M., Kitagawa, J., Matsumoto, S., 2007. Enhanced excitability of nociceptive trigeminal ganglion neurons by satellite glial cytokine following peripheral inflammation. Pain 129, 155–166.

Tandrup, T., Woolf, C.J., Coggeshall, R.E., 2000. Delayed loss of small dorsal root ganglion cells after transection of the rat sciatic nerve. J. Comp. Neurol. 422, 172–180.

Tong, Z., Luo, W., Wang, Y., Yang, F., Han, Y., Li, H., Luo, H., Duan, B., Xu, T., Maoying, Q., Tan, H., Wang, J., Zhao, H., Liu, F., Wan, Y., 2010. Tumor tissue-derived formaldehyde and acidic microenvironment synergistically induce bone cancer pain. PloS. One 5, e10234.

Tu, H., Deng, L., Sun, Q., Yao, L., Han, J.S., Wan, Y., 2004. Hyperpolarization-activated, cyclic nucleotide-gated cation channels: roles in the differential electrophysiological properties of rat primary afferent neurons. J. Neurosci. Res. 76, 713–722.

Vit, J.P., Jasmin, L., Bhargava, A., Ohara, P.T., 2006. Satellite glial cells in the trigeminal ganglion as a determinant of orofacial neuropathic pain. Neuron Glia Biol. 2, 247–257.

Vit, J.P., Ohara, P.T., Bhargava, A., Kelley, K., Jasmin, L., 2008. Silencing the Kir4.1 potassium channel subunit in satellite glial cells of the rat trigeminal ganglion results in pain-like behavior in the absence of nerve injury. J. Neurosci. 28, 4161–4171.

Watkins, L.R., Maier, S.F., 2002. Beyond neurons: evidence that immune and glial cells contribute to pathological pain states. Physiol. Rev. 82, 981–1011.

Wen, Y.R., Suter, M.R., Kawasaki, Y., Huang, J., Pertin, M., Kohno, T., Berde, C.B., Decosterd, I., Ji, R.R., 2007. Nerve conduction blockade in the sciatic nerve prevents but does not reverse the activation of p38 mitogen-activated protein kinase in spinal microglia in the rat spared nerve injury model. Anesthesiology 107, 12–321.

Woodham, P., Anderson, P.N., Nadim, W., Turmaine, M., 1989. Satellite cells surrounding axotomised rat dorsal root ganglion cells increase expression of a GFAP-like protein. Neurosci. Lett. 98, 8–12.

Xie, W., Strong, J.A., Li, H., Zhang, J.M., 2007. Sympathetic sprouting near sensory neurons after nerve injury occurs preferentially on spontaneously active cells and is reduced by early nerve block. J. Neurophysiol. 97, 492–502.

Xie, W., Strong, J.A., Meij, J.T., Zhang, J.M., Yu, L., 2005. Neuropathic pain: early spontaneous afferent activity is the trigger. Pain 116, 243–256.

Xie, W., Strong, J.A., Zhang, J.M., 2009. Early blockade of injured primary sensory afferents reduces glial cell activation in two rat neuropathic pain models. Neuroscience 160, 847–857.

Xing, G.G., Liu, F.Y., Qu, X.X., Han, J.S., Wan, Y., 2007. Long-term synaptic plasticity in the spinal dorsal horn and its modulation by electroacupuncture in rats with neuropathic pain. Exp. Neurol. 208, 323–332.

Xu, J.T., Xin, W.J., Zang, Y., Wu, C.Y., Liu, X.G., 2006. The role of tumor necrosis factor-alpha in the neuropathic pain induced by lumbar 5 ventral root transection in rat. Pain 123, 306–321.

Xu, M., Aita, M., Chavkin, C., 2008a. Partial infraorbital nerve ligation as a model of trigeminal nerve injury in the mouse: behavioral, neural, and glial reactions. J. Pain 9, 1036–1048.

Xu, Q.G., Midha, R., Martinez, J.A., Guo, G.F., Zochodne, D.W., 2008b. Facilitated sprouting in a peripheral nerve injury. Neuroscience 152, 877–887.

Yu, L., Yang, F., Luo, H., Liu, F.Y., Han, J.S., Xing, G.G., Wan, Y., 2008. The role of TRPV1 in different subtypes of dorsal root ganglion neurons in rat chronic inflammatory nociception induced by complete Freund's adjuvant. Mol. Pain 4, 61.

Zhou, X.F., Deng, Y.S., Chie, E., Xue, Q., Zhong, J.H., McLachlan, E.M., Rush, R.A., Xian, C.J., 1999. Satellite-cell-derived nerve growth factor and neurotrophin-3 are involved in noradrenergic sprouting in the dorsal root ganglia following peripheral nerve injury in the rat. Eur. J. Neurosci. 11, 1711–1722.

Zhuang, Z.Y., Wen, Y.R., Zhang, D.R., Borsello, T., Bonny, C., Strichartz, G.R., Decosterd, I., Ji, R.R., 2006. A peptide c-Jun N-terminal kinase (JNK) inhibitor blocks mechanical allodynia after spinal nerve ligation: respective roles of JNK activation in primary sensory neurons and spinal astrocytes for neuropathic pain development and maintenance. J. Neurosci. 26, 3551–3560.

Zimmermann, M., 1983. Ethical guidelines for investigations of experimental pain in conscious animals. Pain 16, 109–110.